DOI: 10.1111/tgis.12586

RESEARCH ARTICLE

Transactions in GIS WILEY

Object-oriented tracking of thematic and spatial behaviors of urban heat islands

Rui Zhu[1,2] | Éric Guilbert[3] | Man Sing Wong[2,4]

[1]Senseable City Laboratory, Singapore-MIT Alliance for Research and Technology, Singapore, Singapore

[2]Department of Land Surveying and Geo-informatics, The Hong Kong Polytechnic University, Hong Kong, China

[3]Department of Geomatics Sciences, Laval University, Québec, Canada

[4]Research Institute for Sustainable Urban Development, The Hong Kong Polytechnic University, Hong Kong, China

Correspondence
Man Sing Wong, Department of Land Surveying and Geo-informatics, The Hong Kong Polytechnic University, 181 Chatham Road South, Hung Hom, Kowloon, Hong Kong, China.
Email: lswong@polyu.edu.hk

Funding information
General Research Fund, Grant/Award Number: 515513

Abstract

Modeling thematic and spatial dynamic behaviors of urban heat islands (UHIs) over time is important for understanding the evolution of this phenomenon to mitigate the warming effect in urban areas. Although previous studies conceptualized that a UHI only has a single life cycle with spatial behaviors, a UHI can be detected to appear and disappear several times periodically in terms of thematic and spatial integrated behaviors. Such multiple behaviors have not yet been illustrated with proof or evidence. This study conceptualizes a UHI as an object which has thematic and spatial behaviors simultaneously and proposes several graphs to depict periodic life-cycle transitions triggered by behaviors. The conceptualized behaviors have been modeled and implemented in an object-relational database management system and temperature readings collected from numerous weather stations were interpolated as temperature images per hour. The results of this study indicate that the model could track the spatial and thematic evolution of UHIs continuously and reveal their periodical patterns and abnormal cases.

1 | INTRODUCTION

An urban heat island (UHI) is an environmental phenomenon in which air/land surface temperatures in urban areas are higher than in surrounding rural areas. The existence of UHIs is a major problem in most metropolitan areas. They cause many adverse effects such as public health deterioration (Ding et al., 2015; Kenney, Craighead, & Alexander, 2014; Morabito, Crisci, & Moriondo, 2012), public security threats (Cohn & Rotton, 2000; Field, 1992; Rotton & Cohn, 2004), and increasing energy consumption (Fung, Lam, Hung, Pang, & Lee, 2006; Papakostas, Mavromatis, & Kyriakis,

 © 2019 John Wiley & Sons Ltd

2010). It is even a more serious problem in rapidly expanding cities, given that the urbanization process is gathering pace. An investigation into the adverse effects and exploring the causative factors of the phenomenon is thus a matter of urgency. It is therefore necessary to track the evolution of UHIs continuously in both thematic (i.e., temperature variations) and spatial (i.e., areal changes and topological transformations) dimensions over a long period.

Previous studies estimated land surface temperature (LST) in describing UHIs and analyzed its correlation with social indicators (Buyantuyev & Wu, 2010), environmental indices (Hu & Brunsell, 2015) and building impacts (Toparlar et al., 2015; Wong & Nichol, 2013; Wong et al., 2016; Yuan & Ng, 2012). Recent studies tend to analyze discrete pixels toward clustering UHIs as interactive objects extracted from thermal images. For example, object-based analysis clustered pixels of thermal infrared images as polygons of objects so that a strong correlation between spatial and thermal attributes (i.e., areal extent and LST) was revealed (Keramitsoglou, Kiranoudis, Ceriola, Weng, & Rajasekar, 2011). However, these studies are incapable of tracking thematic and spatial changes of UHIs simultaneously over a long period. Although some empirical studies have been conducted by analyzing spatio-temporal variation patterns of UHIs based on the interpolation of air temperatures collected from meteorological stations (Kourtidis et al., 2015; Wu, Wang, Cai, Yang, & Li, 2012), it is a challenge to describe instant changes at a fine temporal resolution over a long time period. Thus, a model using spatiotemporal data is needed to determine pixels of thermal images as UHI objects and track the changes of their dynamics through continuous time.

Many studies modeling geographical phenomena as field objects have included variable boundaries determined by other properties (e.g., temporal and thematic properties) related to the field (Goodchild, Yuan, & Cova, 2007). Their dynamics could be represented in a hierarchical framework in which a *sequence* was composed of consecutive *zones* related together in *processes*, and *events* for observing their shape changes and spatial movements from a series of images (McIntosh & Yuan, 2005; Yuan & Hornsby, 2008). For instance, moving behaviors of each object were modeled as a set of semantic *events* such as *departure* and *arrival*, and patterns were constructed from several sequences of the *events* (Hornsby & Cole, 2007). Other models conceptualized spatiotemporal dynamic phenomena as geo-entities in relationships and implemented data structures fitted for computation (Bothwell & Yuan, 2010; Li, Liang, & Wan, 2013; Pultar, Cova, Yuan, & Goodchild, 2010). These approaches provide an appropriate strategy to model the dynamics of UHIs. For example, a series of zones of UHIs which expand continuously can correspond to a sequence.

However, UHI evolutions may involve a single object or several different objects that associate with topological relationships between zones of UHIs. For example, a UHI can contract, split into two parts, and disappear. Conversely, two UHIs can expand and merge into one. Claramunt and Thériault (1995) proposed a series of topological processes describing the behavior of a single object as an expansion or contraction, and behaviors between several objects as splits, unions, or reallocations. Similar models were developed in which objects disappear and reappear because of merging and splitting behaviors (Bothwell & Yuan, 2011; Nixon & Hornsby, 2010; Renolen, 2000). These studies provide an enlightening approach for modeling complex transformations of UHIs. However, they only focus on conceptual modeling, and tracking UHIs needs logistical modeling incorporated into systematically conceptualized UHI behaviors. Furthermore, Del Mondo, Rodríguez, Claramunt, Bravo, and Thibaud (2013) depicted topological transformations in a *graph* composed of a set of nodes and several edges connecting the nodes with certain filiation relationships. Similarly, different graphs will be proposed to develop tracking dynamics of UHIs in our study.

A study has already proposed an object-oriented spatiotemporal framework in modeling the spatial behavior of UHIs (Zhu, Guilbert, & Wong, 2017). Within this framework, a UHI was defined as a two-dimensional field object whose temperatures were equal to or higher than a reference rural temperature. A UHI may experience different sequences, each of which corresponds to a type of spatial behavior. The changes in a UHI can be either internal with area changes or external involving topological transformations with one or several UHIs. In addition, spatial behaviors have been defined by means of two graphs: (a) a zone graph $\mathcal{G}_Z = (\mathcal{Z}, \mathcal{F}_z)$ which denotes a set of zones ($\mathcal{Z}$) as nodes and a set of filiations ($\mathcal{F}_z$) as edges (e.g., spatial behaviors of zones) associated with the zones; and (b) a sequence graph $\mathcal{G}_S = (\mathcal{S}, \mathcal{E}_s)$ which represents a set of sequences ($\mathcal{S}$) that cover area changes or topological transformations ($\mathcal{E}_s$).

However, the aforementioned framework lacks the capability to investigate temperature variations in the UHI extent, since the field was conceptualized and recorded as a homogeneous surface. Temperature distribution in

a real situation within the UHI extent can vary significantly. For example, the temperature of a small area within a UHI may be steady, whereas the temperature of other areas in the same UHI may rise, corresponding to a place with accumulated anthropogenic heat. The UHI may be considered as consisting of several small UHIs if the small areas are identified as UHIs with higher intensity. To have a better investigation into this phenomenon at different thematic intensities, a new definition of UHI will be introduced.

It has been suggested that geographical phenomena may have a periodical process of state transitions between existence and non-existence (Hornsby & Egenhofer, 2000). As an object, a UHI may appear, disappear, and reappear over time. In this respect, the periodicity links a series of existences as a continuous process, in which the life span of UHIs can extend from a few hours to a couple of days. Thus, establishing the periodicity of UHIs for the investigation over long periods becomes very important for our study.

In addition, the above framework cannot track thematic changes in a UHI. This point is vital to clarify evolutionary trends of temperature since they conclusively determine the spatial extent and consequently influence its spatial behavior (Bothwell & Yuan, 2012). For example, an increase in the UHI temperature may lead to the expansion of its spatial extent at nighttime but contraction during the daytime. Therefore, thematic tracking will also be modeled in our study to explore thematic-associated spatial behaviors.

To build a relationship between two zones at two consecutive time instants for computing the proposed spatial behaviors, the above framework only covered the relationship between the overlapping area and the zone in the prior time instant. This may cause a problem that two zones having no significant overlap with each other are still uncertainly determined as associated zones, but the UHI is a localized phenomenon having no significant displacement (Hua & Wang, 2012; Jalan & Sharma, 2014). To solve this problem, a refined method is also necessary.

In summary, this study is original in four respects: (a) a new concept of UHI will be presented in considering the difference between urban and rural air temperatures; (b) periodical processes of UHIs with state transitions will be proposed to allow UHIs to have longer life spans; (c) thematic behaviors as well as UHI graphs will be proposed and modeled to track the changes in a variety of aspects; and (d) a refined and robust computational method will be developed.

The remainder of this article is organized into three sections. Section 2 presents a new conceptual model of UHIs viewed as dynamic objects and emphasizes spatial and thematic behaviors with periodical transitions. Section 3, through an empirical evaluation in a developed spatial database management system, suggests the effectiveness of the proposed model. Finally, Section 4 presents a discussion and conclusions.

2 | CONCEPTUAL AND LOGICAL MODELING

2.1 | UHIs as dynamic objects

During its lifetime, a UHI evolves through different stages. As shown in Figure 1, a UHI occurs at a given time and place if the temperature measured at this location is higher than a reference rural temperature. The *intensity* at a point is defined by this temperature difference (*d*). The UHI is formed when the temperature difference is above a certain threshold, the *magnitude*.

As a temporal phenomenon, a UHI may expand, contract, or remain stable possibly because the intensity increases, decreases, or remains constant over time. This variation in the extent and intensity of the UHI describes its behavior and can be summarized by a series of concepts represented in Figure 2. The behavior can describe a continuous process or a transformation. Continuous processes can be spatial (when they describe a variation of the UHI extent) or thematic (a variation of intensity).

UHIs also exhibit periodic behavior. Since temperature varies periodically, with for example UHI episodes more intense at night or during the summer, UHIs should be allowed to disappear and reappear periodically at the same location. This consideration is helpful in revealing thematic and spatial evolutionary trends of UHIs over longer periods (e.g., months, seasons, or even years). In this regard, a UHI can go through several *active* and *inactive*

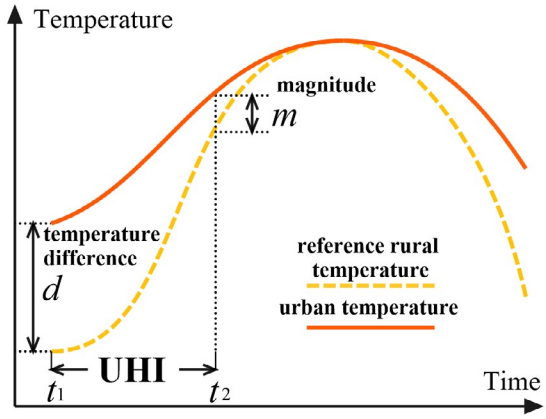

FIGURE 1 A UHI has a temperature at least *m*°C higher than the reference rural air temperature

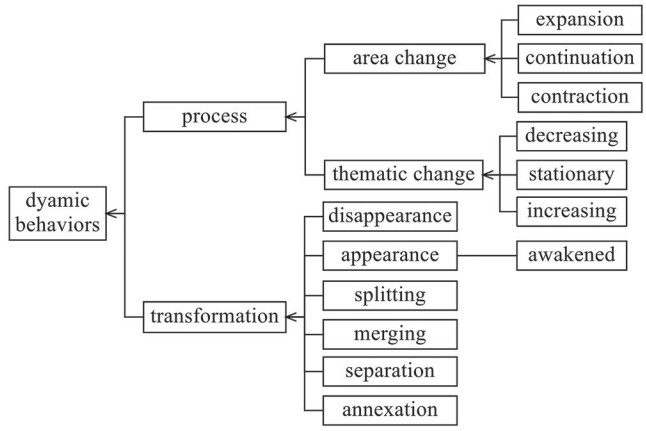

FIGURE 2 A hierarchical set of dynamic behaviors of UHIs

periods (Figure 3). In this scenario, the *appearance* of a UHI indicates a *creation* if it is newly generated and an *activation* if it existed before, and *disappearance* may lead to *death* if it disappears forever.

An active period can start from behaviors when zones appear and terminate at behaviors when zones disappear. However, termination of an *active period* followed by an *inactive period* means that the UHI has disappeared temporarily and will appear again shortly. Therefore, this process requires some topological constraints:

- Zones which have disappeared cannot be made by *annexation* and *merging* since disappearing zones associated with the two behaviors are destroyed forever; and
- activated zones which have been created cannot come from *separation* and *splitting* because both behaviors generate entirely new objects.

2.2 | Graph-based modeling of UHI behaviors

UHIs are observed from temperature data at given time-stamps. At a time-stamp t_i, a UHI u_n is observed by a zone z_n^i where the temperature is above the magnitude. A UHI will have a life span starting at t_i when its first occurrence z_n^i is observed, and ending at t_n^j when its last occurrence is observed. In between, the UHI goes through active and inactive periods and, in each active period, through different sequences characterized by the behaviors of Figure 2. Hence, as in Zhu, Guilbert, et al. (2017), sequences are defined by a series of zones, and relationships between zones and sequences

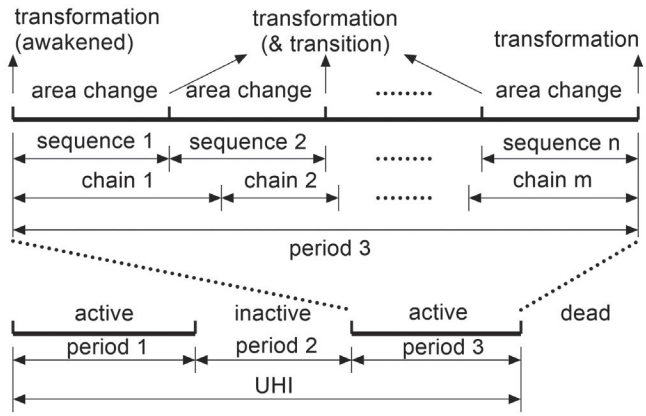

FIGURE 3 Complete life cycle of a UHI. An active period contains a series of sequences and chains, in which a sequence is characterized by a type of spatial behavior associated with transformations, and chains correspond to thematic changes

are defined by a graph. Furthermore, we add a level since a series of sequences form a period. In addition, we consider temperature to define trends in intensity variation.

In order to detect all behaviors, it is first necessary to have the set of all zones identified at all time-stamps $\mathcal{Z}$. A sequence s_n^i is then a series of consecutive zones following the same spatial behavior. As proposed by Zhu, Guilbert, et al. (2017), two graphs are constructed to define the spatial behavior. The zone graph is denoted by $\mathcal{G}_Z = (\mathcal{Z}, \mathcal{F}_z)$, where $(\mathcal{F}_z)$ are edges connecting the zones and corresponding to some ongoing process or transformation. The sequence graph, denoted by $\mathcal{G}_S = (\mathcal{S}, \mathcal{E}_s)$, represents a set of sequences $(\mathcal{S})$ that have areal changes or topological transformations defining the set of edges $(\mathcal{E}_s)$ of $\mathcal{G}_S$.

Similarly, we define a graph storing variations in trends of intensity. The intensity of a UHI can increase, decrease, or remain stationary. A *chain* is defined as a series of zones where the intensity evolves according to a constant trend (Figure 3). Hence, a *chain* can be denoted by $c_n = \{z_n^i, \ldots, z_n^j\}$ where, for any k in $[i{+}1, j]$, variations between $I(z_n^{k-1})$ and $I(z_n^k)$ are of the same kind, where $I(z)$ is the intensity of zone z, equaling the mean value of the temperature differences. Thus, a new graph of chains is introduced, $\mathcal{G}_C = (\mathcal{C}, \mathcal{F}_C)$, where $\mathcal{C}$ is the set of chains and $\mathcal{F}_C$ the filiations between consecutive chains. As with periods, transitions between chains can be defined as follows:

- If $c_n^{i_{j-1}}$ increases and $c_n^{i_j}$ decreases, u_n reaches a *peak* at the transition.
- If $c_n^{i_{j-1}}$ decreases and $c_n^{i_j}$ increases, u_n reaches a *low* at the transition.
- If $c_n^{i_{j-1}}$ increases, $c_n^{i_j}$ stays stationary, and $c_n^{i_{j+1}}$ decreases, chain $c_n^{i_j}$ corresponds to a plateau. u_n is *reaching a plateau* and *leaving a plateau* during the transitions.
- If $c_n^{i_{j-1}}$ decreases, $c_n^{i_j}$ keeps stationary, and $c_n^{i_{j+1}}$ increases, chain $c_n^{i_j}$ is like a floor. u_n is *reaching a floor* and *leaving a floor* during the transitions.
- If both $c_n^{i_{j-1}}$ and $c_n^{i_{j+1}}$ increase or decrease and $c_n^{i_j}$ is stationary, chain $c_n^{i_j}$ represents a pause in the thematic evolution. The two consecutive transitions are *stabilization* and *resumption*.

A series of consecutive sequences or chains starting with an appearance and a disappearance form an *active period*. Similarly, an *inactive period* contains an empty sequence and is denoted by p_n^b so that the reappearance behavior connects with an empty sequence and generates another practical sequence. Thereby, all the periods can be refined into a graph $\mathcal{G}_P = (\mathcal{P}, \mathcal{E}_p)$, where $\mathcal{P}$ is the set of nodes denoting periods and $\mathcal{E}_p$ is the set of edges representing the state transitions between the periods. When several UHIs have interactive evolution in the same urban area or spatial contiguous city clusters, a graph $\mathcal{G}_U = (\mathcal{U}, \mathcal{E}_u)$ can be introduced, where $\mathcal{U}$ is a set of UHIs that makes the graph nodes and $\mathcal{E}_u$ is the edges composed of topological transformations which lead to the creation and destruction of the UHIs. In

summary, three hierarchical graphs have been proposed (Figure 4). Thematic filiations construct the chain graph $\mathcal{G}_C$. $\mathcal{G}_P$ records the complete life cycle of a UHI, which may have several consecutive periods associated with some particular transformations. Ultimately, the entire evolution of a UHI can be finally tracked in $\mathcal{G}_U$.

2.3 | Extraction of UHI changes

The change in a UHI was built up by studying overlapping zones at consecutive time instants. If two zones share a similar position, they most likely belong to the same UHI. Let z^i and z^{i-1} be two zones at consecutive time instants t_i and t_{i-1}. Two irrelevant zones may be associated if only considering the relation between the intersection $z^i \cap z^{i-1}$ and z^{i-1}, because UHIs remain at the same location and do not have significant displacements. Thus, it is more convincing if related zones have a significant intersection $z^i \cap z^{i-1}$ for both z^i and z^{i-1}.

Given two zones z and z', we consider that z significantly overlaps z', and we denote this by $SO(z, z')$, if both zones overlap and the area of their intersection takes a large proportion of the area of z'. Let $0 < \varepsilon < \frac{1}{2}$ be a constant. Then a significant overlap is defined by:

$$SO(z, z') \Leftrightarrow \frac{area(z \cap z')}{area(z')} > 1 - \varepsilon \tag{1}$$

Fixing $\varepsilon < \frac{1}{2}$ guarantees that, for a given zone z', it is not possible to find two disjoint zones significantly overlapping z'. This relation is not symmetrical and the relation $SO(z', z)$ may be false if z is much larger than z'. If both relations are true, both zones significantly overlap, and we denote this relation by $OO(z, z')$, where:

$$OO(z, z') \Leftrightarrow SO(z, z') \wedge SO(z', z) \tag{2}$$

Although a zone cannot be significantly overlapped by two disjoint zones, it can significantly overlap several zones. For a given set of zones Z, the set of all zones significantly overlapped by z is given by:

$$S_Z(z) = \{SO(z, z') | z' \in Z\} \tag{3}$$

For a given zone z, the number of zones in $S_Z(z)$ is given by $\#S_Z(z)$. If Z is the set of all zones $\mathcal{Z}_i$ at time i, we simply write $S_{\mathcal{Z}_i}$ as S^i and its cardinality as $\#S^i$. As zones at a given time instant are supposed to be disjoint, we have:

$$z \in \mathcal{Z}_i, z' \in \mathcal{Z}_i \Rightarrow z \cap z' = \varnothing \tag{4}$$

$$z^i_1 \in \mathcal{Z}_i, z^i_2 \in \mathcal{Z}_i, z^j \in \mathcal{Z}_j \Rightarrow \neg \left(SO(z^i_1, z^j) \wedge SO(z^i_2, z^j)\right) \tag{5}$$

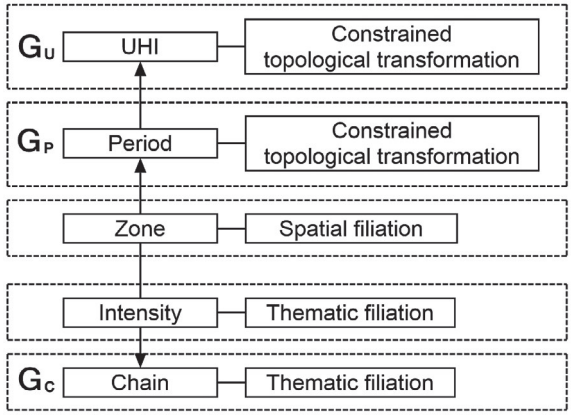

FIGURE 4 Three hierarchical graphs for UHIs

The type of spatial behavior of a UHI can be determined by the number of zones with which it is associated by the type of filiation with these zones. The UHI has area change if it associates with only one zone and without any topological transformations, appearance or disappearance if no overlapping or no association occurs, or transformations when overlapping and associating with several other zones. Thus, spatial behaviors can be conceptualized as *expansion*, *continuation*, or *contraction* if z^i significantly overlaps one zone at t_{i-1}, and the area of z^i is larger, equivalent, or smaller, respectively. In addition, z^i can have topological *appearance* transformations if z^i has no significant overlap between any zones at t_{i-1}, and *disappearance* transformations if z^i has no significant overlap between any zones at t_{i+1}. The other two transformations may occur when more zones are associated:

- *Merge*. z^i overlaps several zones at t_{i-1} and each overlapping area is significant to its corresponding zone at t_{i-1}. If only one overlapping area is exclusively significant to the zone at t_i, the associated zone at t_{i-1} continues as z^i with an *annexation*. Otherwise, a *merge merging* occurs.
- *Split*. Several zones at t_i overlap at z^{i-1} and each overlapping area is significant to its corresponding zone at t_i. If the area of z^{i-1} equals one particular zone at t_i, a *separation* is derived. Otherwise, a *split* occurs.

2.4 | Modeling spatial behaviors

We can now redefine the transitions between zones from their relationships. If a UHI does not undergo any transformation between time t_{i-1} and time t_i, then $\#S^i(z^{i-1})$ and $\#S^{i-1}(z^i)$ cannot be greater than 1. If no change in an area occurs, both zones significantly overlap such that $OO(z^{i-1}, z^i)$ is true. Hence, for two zones $z^{i-1} \in \mathcal{Z}_{i-1}$ and $z^i \in \mathcal{Z}_i$, continuation is defined by:

$$\text{continuation}(z^{i-1}, z^i) \Leftrightarrow OO(z^{i-1}, z^i) \wedge \#S^i(z^{i-1}) = 1 \wedge \#S^{i-1}(z^i) = 1 \tag{6}$$

In a contraction, z^{i-1} is bigger than z^i, hence only $SO(z^{i-1}, z^i)$ is true. As a continuous process, no other zone is involved in the process. Therefore, the contraction is defined by:

$$\text{contraction}(z^{i-1}, z^i) \Leftrightarrow SO(z^{i-1}, z^i) \wedge \#S^i(z^{i-1}) = 0 \wedge \#S^{i-1}(z^i) = 1 \tag{7}$$

Similarly, an expansion is defined by:

$$\text{expansion}(z^{i-1}, z^i) \Leftrightarrow SO(z^i, z^{i-1}) \wedge \#S^i(z^{i-1}) = 1 \wedge \#S^{i-1}(z^i) = 0 \tag{8}$$

Referring to Figure 2, a process (more specifically, for an area change) is a relationship involving a limited number of zones. Anything that is not a process can then be defined as a transformation. The above three relationships correspond to processes where no topological change occurs. A more general relation can be defined relating two consecutive zones that are parts of a continuing process:

$$\text{process}(z^{i-1}, z^i) \Leftrightarrow \left(SO(z^{i-1}, z^i) \vee SO(z^i, z^{i-1})\right) \wedge \max\left(\#S^i(z^{i-1}), \#S^{i-1}(z^i)\right) = 1 \tag{9}$$

Transformations can involve several zones as different UHIs may be engaged. For example, a merge involves a set of zones $Z = \{z_1^{i-1}, \ldots, z_m^{i-1}\} \subset \mathcal{Z}_{i-1}$ and one zone $z^i \in \mathcal{Z}_i$. The zone z^i has to significantly overlap all the zones of Z. However, no zone of $\mathcal{Z}_{i-1}$ significantly overlaps z^i.

$$\text{merging}(Z, z^i) \Leftrightarrow \left(S^{i-1}(z^i)\right) \wedge \left(\forall z \in \mathcal{Z}_{i-1}, \neg SO(z, z^i)\right) \tag{10}$$

In the case where another zone $z_0^{i-1} \in \mathcal{Z}_{i-1}$ significantly overlaps z^i, we have an annexation instead of a merge:

$$\text{annexation}(z_0^{i-1}, Z, z^i) \Leftrightarrow \left(S^{i-1}(z^i)\right) \wedge \left(\forall z \in Z, \neg SO(z, z^i)\right) \wedge SO(z_0^{i-1}, z^i) \tag{11}$$

Conversely, one zone z^{i-1} at t_{i-1} overlapping a set of zones $Z=\{z_1^i,\ldots,z_m^i\}\subset\mathcal{Z}_i$ at t_i corresponds to a split. This requires that z^{i-1} significantly overlaps all the zones of Z while no zone overlaps z^{i-1} significantly:

$$\text{splitting}(z^{i-1},Z)\Leftrightarrow\left(S^i(z^{i-1})\right)\wedge\left(\forall z\in\mathcal{Z}_i,\neg SO(z,z^{i-1})\right) \tag{12}$$

A separation occurs if one zone z_0^i significantly overlaps z^{i-1}:

$$\text{separation}(z^{i-1},Z,z_0^i)\Leftrightarrow\left(S^i(z^{i-1})\right)\wedge\left(\forall z\in Z,\neg SO(z,z^{i-1})\right)\wedge SO(z_0^i,z^{i-1}) \tag{13}$$

Finally, a zone $z^i\in\mathcal{Z}_i$ can appear or disappear at time t_i:

$$\text{appearance}(z^i)\Leftrightarrow\forall z\in\mathcal{Z}_{i-1},\neg\left(SO(z,z^i)\vee SO(z^i,z)\right) \tag{14}$$

$$\text{disappearance}(z^i)\Leftrightarrow\forall z\in\mathcal{Z}_{i+1},\neg\left(SO(z,z^i)\vee SO(z^i,z)\right) \tag{15}$$

In the first case it is not related to any zone in $\mathcal{Z}_{i-1}$. In the second case it is not related to any zone in $\mathcal{Z}_{i+1}$.

Zones would have different spatial behaviors when their overlaps are in different scenarios. For example, if $SO(z_b,z_c)$ and $SO(z_b,z_a)$ are true, we have a merge. Different from the determined relationship $SO(z_b,z_c)$ and $SO(z_a,z_b)$, an annexation could be obtained (Figure 5). We may also have $SO(z_a,z_d)$, which leads to a split. In this case, z_a would have a special behavior, combining a split and a merge at the same time.

2.5 | Modeling thematic behaviors

Thematic behaviors are studied by measuring the evolution of intensity through time. From one instant to the next, it can *increase*, *decrease*, or remain *stationary*:

$$\text{decrease}(z^{i-1},z^i)\Leftrightarrow I(z^{i-1})-I(z^i)>\varepsilon, \tag{16}$$

$$\text{increase}(z^{i-1},z^i)\Leftrightarrow I(z^i)-I(z^{i-1})>\varepsilon, \tag{17}$$

$$\text{stationary}(z^{i-1},z^i)\Leftrightarrow|I(z^{i-1})-I(z^i)|<\varepsilon \tag{18}$$

Indeed, if the intensity remains within a limited range, it reasonable to consider it is *stationary*.

2.6 | Modeling consecutive active periods

Determination of two consecutive active periods connected by an inactive period is necessary to construct a UHI. As conceptualized above, z^i could either derive a creation if it is newly generated or an activation if it has already

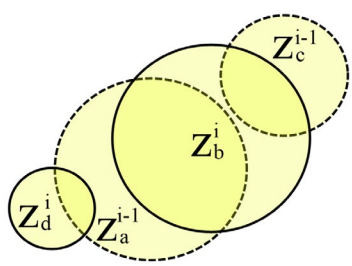

FIGURE 5 Different overlapping scenarios generate different spatial behaviors

existed. When z^i appears, a retrospective trace will check whether there was a disappeared z^{i-x} at the same location. Two active periods can be connected if (z^{i-x}, z^i) are spatially associated:

$$\text{consecutive}(p_n, p'_n) \Leftrightarrow \left(\text{process}(z^{i-x}, z^i) \wedge (x \geqslant 2)\right) \wedge \left(\neg\text{process}(z^{i-y}, z^i) \wedge (\forall y < x)\right) \quad (19)$$

3 | EMPIRICAL EVALUATION

3.1 | Study area and pre-processing

Guangzhou, with its humid subtropical climate, is one of the most urbanized cities in China and has a population of over 13 million. It has high temperatures throughout the year. Since the model requires high temporal resolution of the data set to track changes of UHIs continuously, hourly updated near-surface (approximately 1.5 m above the land surface) air temperatures were measured at 216 automatic weather stations (Figure 6), 159 of which were located in the urban area (3,660 km^2 in size). Major stations in urban areas were on concrete surfaces besides roads and/or buildings. To analyze evolutionary trends of UHIs over a long time, data were collected in the year 2015 over six one-week periods, each separated by an interval of 21 days, from July 31 to August 6, August 28 to September 3, September 25 to October 1, October 23 to 29, November 20 to 26, and December 18 to 24.

To obtain a series of temperature images from the weather stations, a universal kriging interpolation method was used which can highlight "hotspot" regions of UHIs, assuming the input data set is characterized by an overriding trend (Chai et al., 2011; Hofstra, Haylock, New, Jones, & Frei, 2008; Irmak et al., 2010; Stahl, Moore, Floyer, Asplin, & McKendry, 2006). Since weekly averaged root mean square errors for the six weeks were 1.06, 0.99, 1.13, 1.06, 1.07, and 1.03°C, the magnitude m should be notably larger than 1°C to confidently extract zones of

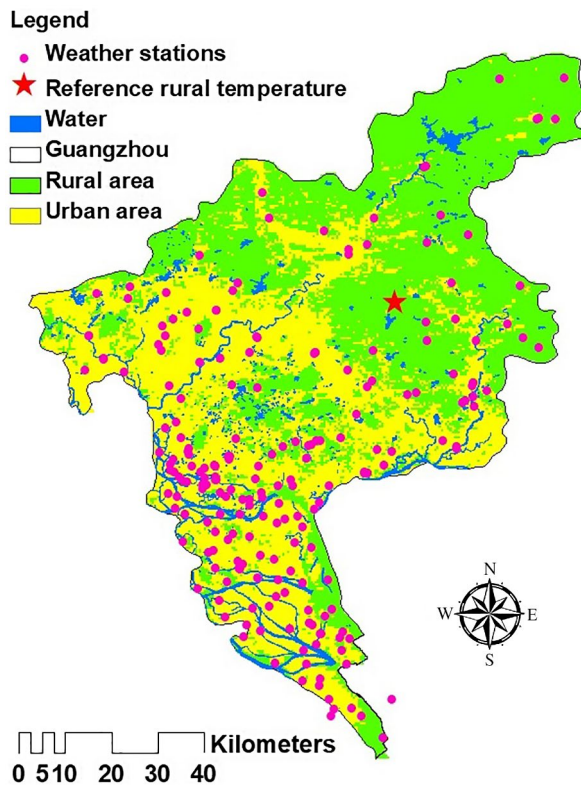

FIGURE 6 Weather stations are predominantly located in the urban areas of Guangzhou

UHIs. Temperatures observed at the star symbol in Figure 6 were located in Dajinfeng Eco-scenic Park, which is a forest area close to urban areas, so they can represent the rural temperatures confidently to extract zones of UHIs and will not be affected by the heat dispersed from urban areas. Also, several other rural stations have lower temperatures so that rural areas may be included as part of a UHI if these stations are used. Therefore, only one rural station was used as the reference for rural temperatures to extract zones of UHIs.

3.2 | System implementation

The model was implemented in PostgreSQL 10 to simulate behaviors and to track their changes during the complete life cycles of UHIs. A UML model is presented in Figure 7, which summarizes the classes as discrete records in tables and represents their associations. First, a time series of temperature images generated hourly from air temperatures is compiled in a set of `image` tables. Hence, all the zones are extracted from temperature images, and their spatial and thematic information is tabulated in the `zone` table. For example, each row records a unique zone identified by its ID (`zid`), which exists as a single polygon (`shape`) at a time-stamp (`t_s`). Temperatures in the `shape` polygon are at least a magnitude `m` higher than the reference rural temperature (`rural_t`). In particular, four types of thermal intensities are also summarized (`max_t`, `min_t`, `mea_t`, and `mod_t`). In order to determine filiation relations between zones, overlapping areas (`overlap_area`) of zones at the current instant (`czid`) and zones in the previous instant (`pzid`) should be calculated in advance. To avoid duplicate calculation, zones with area changes and topological transformations are classified into three tables (`merge`, `split`, and `area_change`) such that the `behavior` table can be built as the central domain to describe two types of behaviors (`spb` and `thb`) at each time-stamp (`t_s`). Thus, UHIs (`oid`) can be constructed in the `uhi` table, and each UHI can have one or several periods (`pid`), and each

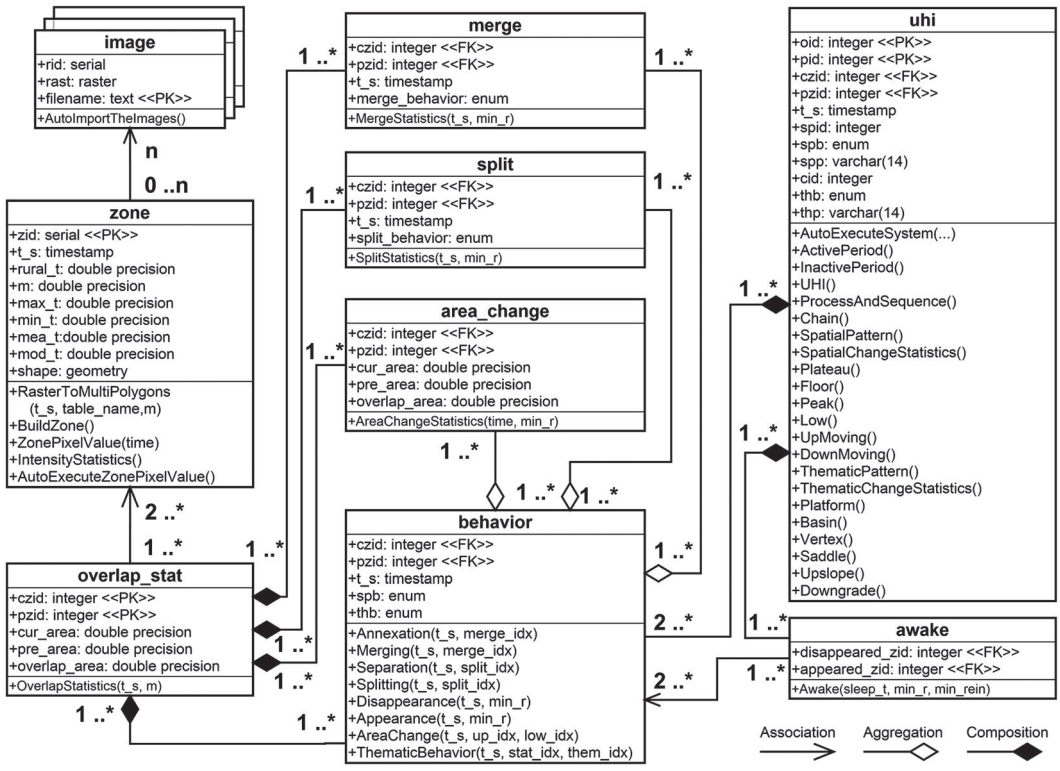

FIGURE 7 A UML model to present database tables, functions, and their associations and generations for tracking spatial and thematic behaviors of UHIs over time

LISTING 1 FUNCTION ActivePeriod()

```
INSERT INTO period(pid, t_s, czid, pzid, spb, thb)
SELECT max(path) AS path, per.t_s, per.czid, per.pzid, per.spb, per.thb
FROM  (WITH RECURSIVE per_u(path, t_s, czid, pzid, spb, thb)
       AS  (SELECT row_number() OVER (ORDER BY t_s) AS path, root.t_s,
                   root.czid, root.pzid, root.spb, root.thb
            FROM   behavior AS root UNION
            SELECT leaf.path, root.t_s, root.czid, root.pzid, root.spb, root.thb
            FROM   behavior AS root, per_u AS leaf
            WHERE  root.czid = leaf.pzid
            AND    leaf.pzid > 0 AND leaf.spat_beh <> 'separa_d_obj'
            AND    root.spb <> 'annexa_d_obj'
            AND    root.spb <> 'merging' AND root.spat_beh <> 'splitting')
      SELECT * FROM per_u ORDER BY path, t_s) AS per
GROUP BY per.t_s, per.czid, per.pzid, per.spb, per.thb;
```

LISTING 2 FUNCTION Awake(sleep_t, min_r, min_rein)

```
INSERT INTO awake(disappeared_zid, appeared_zid)
SELECT tail_seq.zid AS disap_z, head_seq.zid AS reapp_z,
      (head_seq.t_s - tail_seq.t_s) AS dth_t,
       ST_Area(ST_Intersection(head_seq.geom, tail_seq.geom)) AS i_a
FROM  (SELECT zone.* FROM zone, period
       WHERE  spb = 'appearance' AND zone.zid = period.czid) AS head_seq,
      (SELECT zone.* FROM zone, period
       WHERE  spb = 'disappearance' AND zone.zid = period.pzid) AS tail_seq
WHERE  head_seq.t_s - tail_seq.t_s <= sleep_t * 3600 * '1 second'::INTERVAL
AND   head_seq.t_s - tail_seq.t_s >= 2 * 3600 * '1 second'::INTERVAL
AND   ST_Area(ST_Intersection(head_seq.geom, tail_seq.geom))/ST_Area(head_seq.geom) >= min_r
AND   ST_Area(ST_Intersection(head_seq.geom, tail_seq.geom))/ST_Area(tail_seq.geom) >= min_r
AND   ST_Area(ST_Intersection(head_seq.geom, tail_seq.geom))/ST_Area(head_seq.geom) >= min_rein;

INSERT INTO awake(disappeared_zid, appeared_zid)
SELECT cand.disap_z, cand.reapp_z
FROM   awakened_cand AS cand,
      (SELECT cand.reapp_z, min(cand.dth_t) AS min_dth_t
       FROM   awakened_cand AS cand,
             (SELECT min(dth_t) AS min_dth_t, disap_z
              FROM   awakened_cand GROUP BY disap_z) AS dth_cand,
             (SELECT max(i_a) AS max_i_a, dth_t, disap_z
              FROM   awakened_cand GROUP BY disap_z, dth_t) AS ints_cand
       WHERE dth_cand.min_dth_t = cand.dth_t AND dth_cand.disap_z = cand.disap_z
       AND   ints_cand.max_i_a = cand.i_a AND ints_cand.disap_z = cand.disap_z
       AND   dth_cand.disap_z = ints_cand.disap_z GROUP BY cand.reapp_z) AS uhi_cand
WHERE  cand.reapp_z = uhi_cand.reapp_z
AND    cand.dth_t = uhi_cand.min_dth_t;
```

period combines a time series of spatial behaviors determined by thematic behaviors. Simultaneously, sequence and process descriptions for spatial behaviors (`spid`) and thematic behaviors (`cid`) are obtained, and their corresponding patterns (`spp` and `thp`) are finally shown.

It is necessary to identify topological relations associated with zones that can create and destroy an active period (Listing 1). It is also vital to connect active periods that belong to the same UHI by determining awakened zones that trigger new periods (Listing 2). In Listing 1, lines 4–6 generate serial numbers as candidates of period IDs and determine the first zone behavior (`root`) in the periods. Lines 7–12 build continual zone behaviors that extend from the roots (called `leaf`). More specifically, line 9 connects the leaves to the root. Line 10 avoids endless loop computation by ensuring that the appearance and disappearance behaviors are included in the period, and generates new periods when zones are separated as different objects. Lines 11–12 cut off the extension of leaves when zones are destroyed. Finally, lines 3–13 execute the recursive computation and lines 2–14 select the maximum value of path used as the final period ID. In Listing 2, lines 5–6 and 7–8 list zones having *appearance* as the head and *disappearance* as the tail respectively, where time interval between them is more than 2 hr but no longer than the maximum awakened time (lines 9–10). Thus, pairs of heads and tails that satisfy the awakened condition (lines 11–13) are selected as the awakened candidates (lines 2–3). However, several zones that disappeared can map to the same appeared zone in the awakened candidates. On the basis of the candidates which have the minimum sleeping time (lines 19–20), zones having the maximum overlapping area are selected (lines 21–22) from the records of awakened candidates (lines 23–25). Finally, zones satisfying all the conditions are inserted into the awake table (lines 14–27).

3.3 | Results

3.3.1 | Dynamic behaviors of UHIs

Figure 8 presents seven consecutive days of intensities (i.e., the mean value of temperature differences at each time instant) in five different magnitudes. Intensities (with the condition of m = 1°C) lasting almost all the time suggest that m = 1°C cannot distinguish temperature difference effectively. It proves that zones of UHIs should satisfy the condition of m > 1 °C, as suggested in Section 3.1. Over 7 days, intensities for each magnitude increased gradually, and the reference rural temperature also increased from 27.6 to 29.2°C. This reveals that air temperatures in urban areas increase faster than those of the reference rural temperature in this time period, suggesting a typical UHI phenomenon during the summertime. The figure also shows that intensities having a larger m were more stable and of shorter *active* period. For example, the highest peak of the intensities occurred at midnight on August 5 when m = 2°C, while the peak was faded when m = 5°C. This suggests that a small m would help to describe the overall evolutionary trend of UHIs, while a large one might be able to locate stable heat sources of UHIs.

Based on the above statistics, Figure 9 draws UHIs in three magnitudes and presents behaviors of three UHIs queried in the `uhi` table, with object IDs (the `oid` column) of 15 (m = 2°C), 17 (m=3°C), and 10091 (m = 4°C). This shows that the UHI having the largest magnitude contracted insignificantly without any topological transformation and the intensity was stationary throughout the night. Since this UHI was located in the densest urban area of Guangzhou, it could have been formed by many phenomena, such as heat exhaust from factories and vehicles, the release of household energy, and heat storage from building infrastructures, so that they can release the heat continuously and stably at nighttime. Correspondingly, the UHI with a moderate magnitude contracted by separating several parts from its origin continuously, and the intensity decreased gradually. New UHIs occurred from the separation simultaneously. Urban temperatures outside the downtown area decreased faster than the reference rural temperature, leading to a decrease in the intensity and contraction of the zone during the night from 2 to 4 a.m. Then the air started to accumulate heat at dawn from 5 to 6 a.m. so that air temperatures increased faster than the reference rural temperature, leading to expansion and merging. Finally, UHIs contracted and disappeared at sunrise (7 a.m.) because the reference rural temperature increased faster and temperature differences were smaller than m=3°C. In contrast, the UHI with the smallest magnitude expanded gradually before dawn but

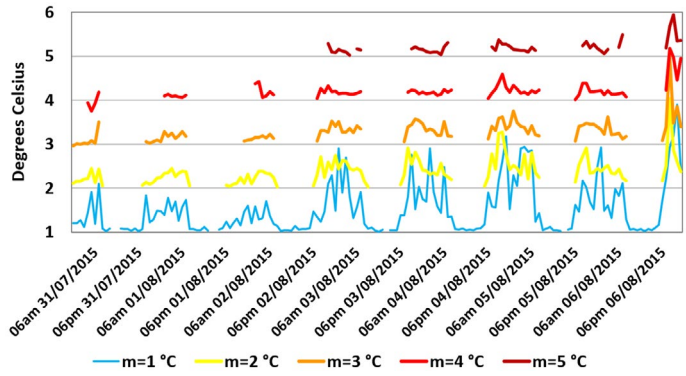

FIGURE 8 Intensities of UHIs in five different magnitudes for seven consecutive days

contracted dramatically at dawn, and finally disappeared in the early morning. The intensity had a contrary evolutionary trend at the same time, which decreased and increased continuously followed by the other decrease. This suggests that UHIs in different magnitudes have different evolutions.

Additionally, a UHI can exist throughout several periods (i.e., two active periods are connected by an inactive period in the `pid` column) as presented in Figure 9. This means that the UHI can either reappear the next day (for the UHI with `oid` = 15) or in several days (for the UHI with `oid` = 17). This reveals that UHIs have periodicities and demonstrates that the proposed model can track evolutions of UHIs over a longer time compared with previous models by establishing the periodicity.

3.3.2 | Thematic evolution of UHIs

To find evolutionary trends of UHIs over seasons, the study investigated changes of UHIs during six one-week periods over 6 months from July to December in 2015 (Figure 10). This shows that UHIs mostly happened and were the most significant at night. However, an entirely different phenomenon is found that UHIs were the most significant at noon on September 30, October 27 and November 25. This abnormal phenomenon always occurred with a dramatic decrease in the reference rural temperatures when it was sunny on the previous day and raining or cloudy on the current day. The explanation is that heat accumulated on the previous day could not disperse immediately at night because of the thermal insulation contributed by the urban canopy, that is, rain-rich clouds obstructed the spread of heat. Heat accumulated on the previous day is gradually released on the following day so that the UHI could have a higher intensity with additional heat resources from anthropogenic heat fluxes (e.g., heat emissions from vehicles) in the daytime.

Some of our findings are also shown in Figure 10. UHIs usually occur at night and UHIs with larger magnitudes are more stable with a shorter active period. However, intensities in dense urban areas (m = 4°C) can grow dramatically, reaching up to 5.5°C at dawn on September 25 and November 23, making them extremely significant. This phenomenon is always accompanied by clear sky at night followed by sunshine at dawn. This suggests that continuously clear sky would likely generate significant UHIs. The explanation is that dense urban areas can release a larger amount of heat rapidly at night with a clear sky so that air temperatures in urban areas can increase much faster at dawn, even though reference rural temperatures increase dramatically. In contrast , UHIs were insignificant and might not even happen when amplitudes of the reference rural temperatures became much smaller between December 20 and December 23, caused by thick fog throughout each day. A similar phenomenon occurred between August 28 and September 3 when UHIs were short and insignificant over the whole week. However, the mechanism is different, because the heat was dispersed by a rainstorm lasting the whole week and clouds obstructed absorption of solar radiation fluxes from the land surface. Moreover, continuous rain (e.g., between August 28 and September 3) and fog (e.g., between December 20 and December 23) could obstruct the

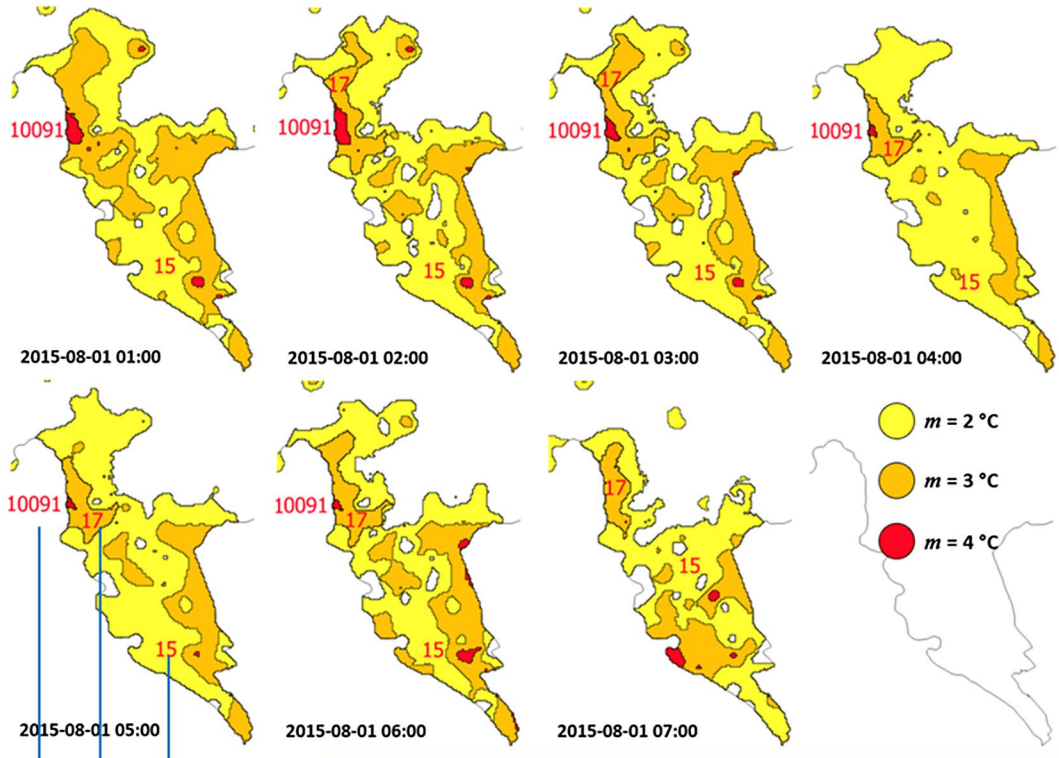

oid	pid	t_s	czid	pzid	spid	spb	spp	cid	thb	thp
15	315	31/7/2015 21:00	512	500	171	annex		159	stationary	
15	315	31/7/2015 22:00	41	512	171	annex		164	decreasing	re_low
15	315	31/7/2015 23:00	56	41	171	annex		186	increasing	le_low
15	315	1/8/2015 0:00	524	56	171	annex		186	increasing	le_low
15	315	1/8/2015 1:00	408	524	249	expan	re_peak	186	increasing	le_low
15	315	1/8/2015 2:00	414	408	250	contr	le_peak	213	decreasing	downgrade
15	315	1/8/2015 3:00	247	414	258	annex		217	stationary	stabilization
15	315	1/8/2015 4:00	533	247	266	contr		221	decreasing	downgrade
15	315	1/8/2015 5:00	537	533	272	annex		227	increasing	re_peak
15	315	1/8/2015 6:00	65	537	272	annex		227	increasing	re_peak
15	315	1/8/2015 7:00	542	65	272	annex		247	decreasing	le_peak
15	315	1/8/2015 8:00	403	542	295	contr		247	decreasing	le_peak
15	315	1/8/2015 9:00	0	403	300	disap		250	null	
15	316	1/8/2015 10:00								
15	316	1/8/2015 22:00								
15	431	1/8/2015 23:00	564	0	346	appea		294	null	
15	431	2/8/2015 0:00	593	564	360	expan		312	increasing	upslope
15	431	2/8/2015 1:00	583	593	360	expan		315	stationary	stabilization
15	431	2/8/2015 2:00	370	583	398	merge		335	increasing	upslope
17	289	1/8/2015 2:00	350	334	178	separ		171	increasing	re_peak
17	289	1/8/2015 3:00	361	350	209	annex		184	decreasing	le_peak
17	289	1/8/2015 4:00	304	361	213	separ		199	stationary	
17	289	1/8/2015 5:00	371	304	241	expan		199	stationary	
17	289	1/8/2015 6:00	384	371	254	annex		216	decreasing	
17	289	1/8/2015 7:00	387	384	272	contr		216	decreasing	
17	289	1/8/2015 8:00	0	387	283	disap		243	null	
17	290	1/8/2015 9:00								
17	290	6/8/2015 17:00								
17	1288	6/8/2015 18:00	627	0	1217	appea		1104	null	
17	1288	6/8/2015 19:00	826	627	1229	merge		1110	increasing	
10091	91	1/8/2015 1:00	112	0	55	appea		30	null	
10091	91	1/8/2015 2:00	121	112	64	annex		35	stationary	
10091	91	1/8/2015 3:00	71	121	67	contr	re_low	35	stationary	
10091	91	1/8/2015 4:00	72	71	67	contr	re_low	35	stationary	
10091	91	1/8/2015 5:00	74	72	67	contr	re_low	35	stationary	
10091	91	1/8/2015 6:00	80	74	84	expan	le_low	35	stationary	
10091	91	1/8/2015 7:00	0	80	90	disap		61	null	

FIGURE 9 Behaviors of UHIs in three magnitudes of 2, 3, and 4°C

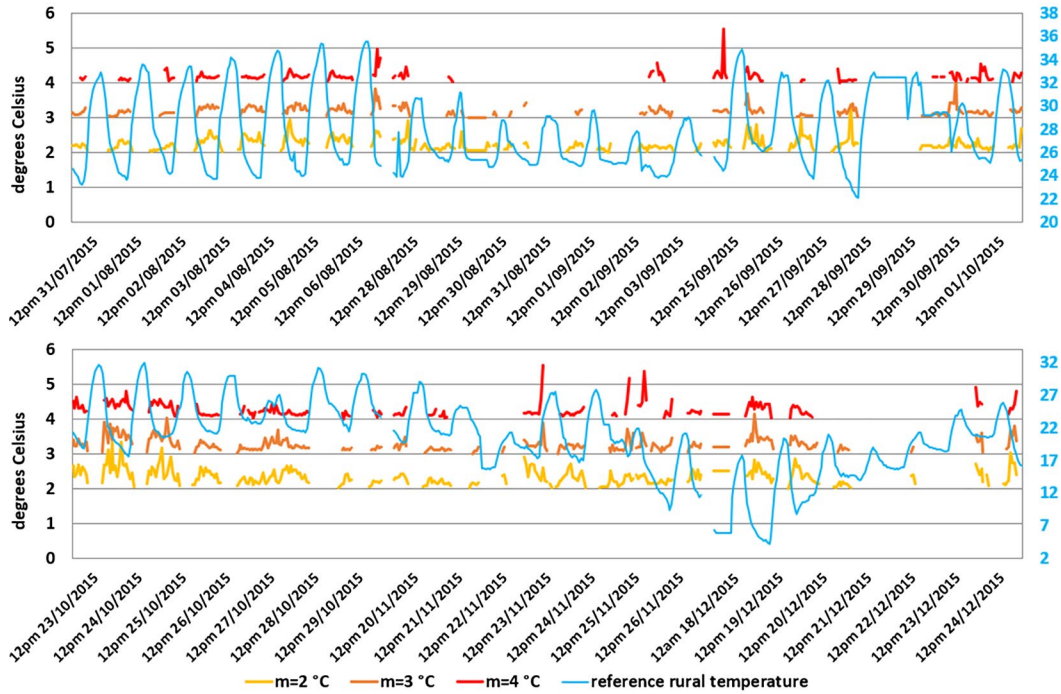

FIGURE 10 Intensities in three magnitudes over 6 weeks, together with the reference rural temperatures

occurrence of UHIs. Apparently observed from these weather patterns, daily duration and intensities of UHIs were almost the same from summer to winter, disregarding the seasonal difference.

3.3.3 | Relationship of UHIs in different magnitudes

According to the proposed UHI definition, a UHI in a small magnitude would be more likely to occur within a large zone, so that zones with a large magnitude can locate in the same zone with a small magnitude. Based on the evidence that small and dense urban areas can accumulate a great amount of heat from solar heat fluxes (Nichol, Fung, Lam, & Wong, 2009) and anthropogenic heat fluxes (Zhu, Wong, Guilbert, & Chan, 2017), there are reasons to believe that dense urban areas could be the largest heat resource in a city. Thus, correlation analysis between areas of zones in the same instant but in different magnitudes would help to explore the relationship of UHIs in different magnitudes.

Total areas of UHIs in three magnitudes (m = 2, 3, 4°C) were computed through SQL queries and then correlations of the total areas between m = 3, 4°C (Figure 11) and between m = 2, 4°C (Figure 12) were computed respectively by using R^2. Overall, R^2 = 0.78 for m=3, 4°C and R^2 = 0.59 for m = 2, 4°C for all the six weeks. Both cases show positive correlations. These two figures also show that total areas of UHIs were several times (for m = 3°C) to dozens of times (for m = 2°C) larger those that in a large magnitude (m = 4°C).

In particular, all the values of R^2 for m = 3, 4°C were larger than 0.80 except for those during the 7 days between September 25 and October 1 (Figure 11). These values show strong and positive correlations. There are two possible reasons. First, dense urban areas determined the evolution of UHIs when m = 4°C, since the urban areas and zones of the UHIs had significant overlap most of the time. Second, a great amount of the heat generated in small and dense urban areas could diffuse to large and low-density urban areas through air thermal diffusion. This process fundamentally affected thermal distribution in low-density urban areas and thus led to merging and annexation between zones, as presented in Figure 9. This reasoning can explain why strong and

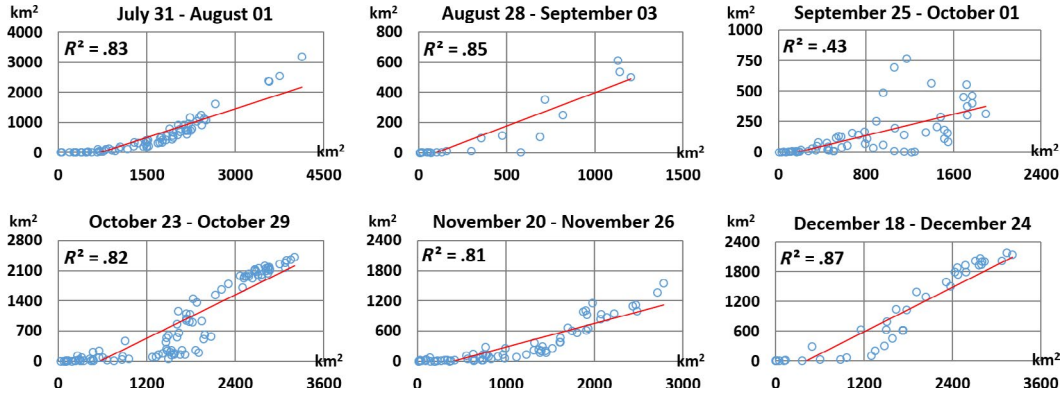

FIGURE 11 Correlation analysis between areas of UHIs in m = 3°C (x-axis) and m = 4°C (y-axis) over 6 weeks

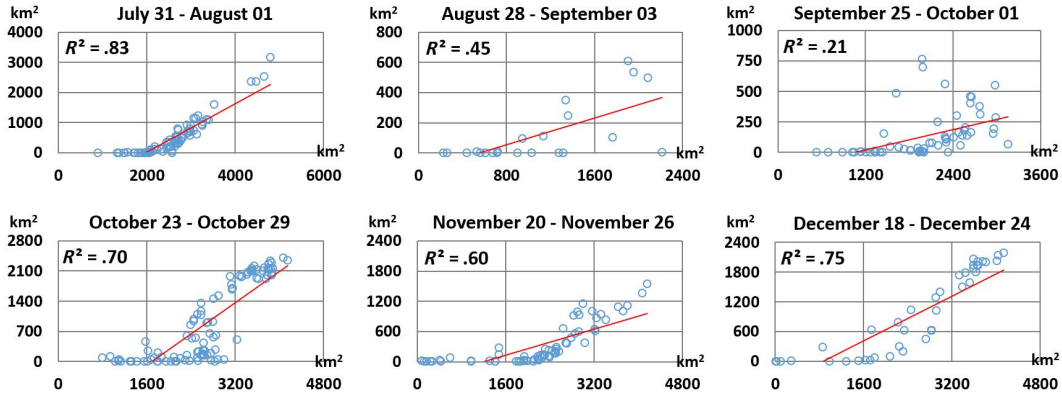

FIGURE 12 Correlation analysis between areas of UHIs in m=2°C (x-axis) and m=4°C (y-axis) over 6 weeks

positive correlations could be shown between areas of zones. Therefore, UHIs of a large magnitude (m = 4°C) could overwhelmingly influence evolution of UHIs of a small magnitude (m = 3°C).

Additionally, the influence could extend across different seasons because it was maintained from August to December for $R^2 \geq 0.80$ overall. There is a weak and positive correlation (R^2 = 0.43) in the period between September 25 and October 1. Given the fact that the weather was changing during these days, that is, with a mixture of fog, cloud, and sunshine due to different meteorological conditions, it can be deduced that unstable weather can impede heat absorption and thermal diffusion, leading to the disappearance of UHIs.

Even though all the values of R^2 for m = 2, 4°C (Figure 12) were smaller than those for m = 3, 4°C (Figure 11), all of them show a positive correlation. Surprisingly, strong and positive correlations remained ($R^2 \geq 0.70$) between July 31 and August 1, between October 23 and October 29, and between December 18 and December 24 for UHIs in m = 2, 4°C. The explanation is that heat from small and dense urban areas still could influence the evolution of UHIs, spreading into much larger areas in mixed urban–rural regions.

4 | DISCUSSION AND CONCLUSIONS

This study established an object-oriented data model organized by graphing in three hierarchies. The model allows tracking of thematic and spatial behaviors of UHIs. Instead of focusing on numeric air temperatures of UHIs, this

study proposed the concept of *intensity* as the statistics of temperature differences between urban temperatures and reference rural temperatures to build a model of different behaviors.

A UHI has a *magnitude* to maintain its significance, and each one may experience several transitions between active and inactive periods, which breaks the traditional bondage of tracking UHIs in discrete days and allows continuous tracking over days, weeks, and even seasons. UHIs at different magnitudes may build inclusive relationships with each other, which means that a large UHI may contain several small UHIs with a large magnitude. As such, the small UHIs would experience active and inactive transitions when the large UHI is active, while the disappearance of the large UHI would lead to the disappearance of all small ones.

A simple and effective criterion to test the reliability of the model is based on the notion that each zone has only one behavior at each time instant (no duplicate or undetermined behaviors). The model has been evaluated through a set of input parameters and a complete set of 6 weeks of data. Several technologies were used in the database management system to accelerate the computation, such as creating indices in spatial and non-spatial columns, tabulating intermediate data maintained in RAM, and creating a new table to replace an existing one instead of making UPDATE queries. Through these optimizations, computing all the behaviors and establishing all the proposed graphs require about 3 min.

This study has two limitations. First, the spatial density of the stations is not high enough, so that micro-changes at the street/block level are difficult to detect. Second, a UHI undergoes either topological transformation or areal change at each time instant. However, an existing UHI should have both spatial and thematic properties all the time so that correlations between areas and temperatures for UHIs can be determined continuously. Future work could allow a UHI to have areal change and topological transformation at a time instant if the UHI is still active. This study omitted displacements of UHIs as most of them are locationally static. Future work could incorporate this model into other geographical phenomena with obvious displacements, such as water pollution. The model could thus be improved in a more sophisticated scenario.

Four important findings in this study can be summarized, and they point to the effectiveness of the model. Firstly, clear sky at night followed by sunshine at dawn can promote the occurrence of UHIs of extremely high intensities at dawn. Secondly, UHIs in a specific magnitude could maintain their intensities during the daytime not only in summer but also across winter without the influence of rainy and foggy weather. Thirdly, UHIs normally occur at night across different seasons, while they can also be very significant at noon because of the weather changes from sunny to rainy/cloudy on two consecutive days. Finally, UHIs in a larger magnitude are more readily associated with locations with smaller spatial extents and shorter duration of active periods.

To sum up, two conclusions can be drawn. First, our model is original in four respects since we proposed: (a) a new definition for investigating UHIs of varying significance; (b) a new transition between active and inactive periods to extend the life span of UHIs; (c) a new UHI graph concept to track dynamics of UHIs; and (d) a new method to confidently compute spatial behaviors. Second, based on a well-designed database management system, the empirical evaluation suggests that the proposed model can process a large set of images and can allow queries to explore evolution and characteristics of UHIs effectively.

ACKNOWLEDGEMENTS

This work was supported in part by the General Research Fund (Project ID: 515513) of the Research Grants Council of Hong Kong. The authors are also grateful for support from National Research Foundation Singapore (NRFS) and Singapore-MIT Alliance for Research and Technology (SMART).

ORCID


Man Sing Wong https://orcid.org/0000-0002-6439-6775

REFERENCES

Bothwell, J., & Yuan, M. (2010). Apply concepts of fluid kinematics to represent continuous space-time fields in temporal GIS. *Annals of GIS*, *16*(1), 27–41.

Bothwell, J., & Yuan, M. (2011). A kinematics-based GIS methodology to represent and analyze spatiotemporal patterns of precipitation change in the IPCC A2 scenario. In *Proceedings of the 19th ACM SIGSPATIAL International Conference on Advances in Geographic Information Systems* (pp. 152–161). Chicago, IL: ACM.

Bothwell, J., & Yuan, M. (2012). A spatiotemporal GIS framework applied to the analysis of changes in temperature patterns. *Transactions in GIS*, *16*(6), 901–919.

Buyantuyev, A., & Wu, J. (2010). Urban heat islands and landscape heterogeneity: Linking spatiotemporal variations in surface temperatures to land-cover and socioeconomic patterns. *Landscape Ecology*, *25*(1), 17–33.

Chai, H. X., Cheng, W. M., Zhou, C. Q., Chen, X., Ma, X. Y., & Zhao, S. M. (2011). Analysis and comparison of spatial interpolation methods for temperature data in Xinjiang Uygur Autonomous Region, China. *Natural Science*, *3*(12), 999–1010.

Claramunt C., & Thériault M. (1995). Managing time in GIS: An event-oriented approach. In J. Clifford & A. Tuzhilin (Eds.), *Recent advances in temporal databases. Workshops in computing* (pp. 23–42). London, UK: Springer.

Cohn, E. G., & Rotton, J. (2000). Weather, seasonal trends and property crimes in Minneapolis, 1987–1988. A moderator-variable time-series analysis of routine activities. *Journal of Environmental Psychology*, *20*(3), 257–272.

Del Mondo, G., Rodríguez, M. A., Claramunt, C., Bravo, L., & Thibaud, R. (2013). Modelling consistency of spatio-temporal graphs. *Data & Knowledge Engineering*, *84*, 59–80.

Ding, Z., Guo, P., Xie, F., Chu, H., Li, K., Pu, J., … Zhang, Q. (2015). Impact of diurnal temperature range on mortality in a high plateau area in southwest China: A time series analysis. *Science of the Total Environment*, *526*, 358–365.

Field, S. (1992). The effect of temperature on crime. *British Journal of Criminology*, *32*(3), 340–351.

Fung, W. Y., Lam, K. S., Hung, W. T., Pang, S. W., & Lee, Y. L. (2006). Impact of urban temperature on energy consumption of Hong Kong. *Energy*, *31*(14), 2623–2637.

Goodchild, M. F., Yuan, M., & Cova, T. J. (2007). Towards a general theory of geographic representation in GIS. *International Journal of Geographical Information Science*, *21*(3), 239–260.

Hofstra, N., Haylock, M., New, M., Jones, P., & Frei, C. (2008). Comparison of six methods for the interpolation of daily, European climate data. *Journal of Geographical Research*, *113*, D21110.

Hornsby, K., & Egenhofer, M. J. (2000). Identity-based change: A foundation for spatio-temporal knowledge representation. *International Journal of Geographical Information Science*, *14*(3), 207–480.

Hornsby, K. S., & Cole, S. (2007). Modeling moving geospatial objects from an event-based perspective. *Transactions in GIS*, *11*(4), 555–573.

Hu, L., & Brunsell, N. A. (2015). A new perspective to assess the urban heat island through remotely sensed atmospheric profiles. *Remote Sensing of Environment*, *158*, 393–406.

Hua, L., & Wang, M. (2012). Temporal and spatial characteristics of urban heat island of an estuary city, China. *Journal of Computers*, *7*(12), 3082–3087.

Irmak, A., Ranade, P. K., Marx, D., Irmak, S., Hubbard, K. G., Meyer, G. E., & Martin, D. L. (2010). Spatial Interpolation of climate variables in Nebraska. *Transactions of the American Society of Agricultural & Biological Engineers*, *53*(6), 1759–1771.

Jalan, S., & Sharma, K. (2014). Spatio-temporal assessment of land use/land cover dynamics and urban heat island of Jaipur city using satellite data. *International Archives of the Photogrammetry, Remote Sensing & Spatial Information Sciences*, *60*(8), 767–772.

Kenney, W. L., Craighead, D. H., & Alexander, L. M. (2014). Heat waves, aging, and human cardiovascular health. *Medicine and Science in Sports & Exercise*, *46*(10), 1891–1899.

Keramitsoglou, I., Kiranoudis, C. T., Ceriola, G., Weng, Q., & Rajasekar, U. (2011). Identification and analysis of urban surface temperature patterns in Greater Athens, Greece, using MODIS imagery. *Remote Sensing of Environment*, *115*(12), 3080–3090.

Kourtidis, K., Georgoulias, A. K., Rapsomanikis, S., Amiridis, V., Keramitsoglou, I., Hooyberghs, H., … Melas, D. (2015). A study of the hourly variability of the urban heat island effect in the Greater Athens area during summer. *Science of the Total Environment*, *517*, 162–177.

Li, J., Liang, Y., & Wan, J. (2013). Geo-ontology-based object-oriented spatiotemporal data modeling. In Q. Zu, B. Hu, & A. Elçi (Eds.), *Pervasive computing and the networked world: ICPCA/SWS 2012* (Lecture Notes in Computer Science, Vol. *7719*, pp. 302–317). Berlin, Germany: Springer.

McIntosh, J., & Yuan, M. (2005). Assessing similarity of geographic processes and events. *Transactions in GIS*, *9*(2), 223–245.

Morabito, M., Crisci, A., & Moriondo, M. (2012). Air temperature-related human health outcomes: Current impact and estimations of future risks in Central Italy. *Science of the Total Environment*, *441*, 28–40.

Nichol, J. E., Fung, W. Y., Lam K. S., & Wong, M. S. (2009). Urban heat island diagnosis using ASTER satellite images and 'in situ' air temperature. *Atmospheric Research*, *94*(2), 276–284.

Nixon, V., & Hornsby, K. S. (2010). Using geolifespans to model dynamic geographic domains. *International Journal of Geographical Information Science*, *24*(9), 1289–1308.

Papakostas, K., Mavromatis, T., & Kyriakis, N. (2010). Impact of the ambient temperature rise on the energy consumption for heating and cooling in residential buildings of Greece. *Renewable Energy*, *35*(7), 1376–1379.

Pultar, E., Cova, T. J., Yuan, M., & Goodchild, M. F. (2010). EDGIS: A dynamic GIS based on space-time points. *International Journal of Geographical Information Science*, *24*(3), 329–346.

Renolen, A. (2000). Modelling the real world: Conceptual modelling in spatiotemporal information system design. *Transactions in GIS*, *4*(1), 23–42.

Rotton, J., & Cohn, E. G. (2004). Outdoor temperature, climate control, and criminal assault. *Environment & Behavior*, *36*(2), 276–306.

Stahl, K., Moore, R. D., Floyer, J. A., Asplin, M. G., & McKendry, I. G. (2006). Comparison of approaches for spatial interpolation of daily air temperature in a large region with complex topography and highly variable station density. *Agricultural & Forest Meteorology*, *139*, 224–236.

Toparlar, Y., Blocken, B., Vos, P., Heijst, G. J. F., Janssen, W. D., Hooff, T., … Immermans, H. J. P. (2015). CFD simulation and validation of urban microclimate: A case study for Bergpolder Zuid, Rotterdam. *Building & Environment*, *83*, 79–90.

Wong, M. S., & Nichol, J. E. (2013). Spatial variability of frontal area index and its relationship with urban heat island intensity. *International Journal of Remote Sensing*, *34*(3), 885–896.

Wong, M. S., Zhu, R., Liu, Z., Lu, L., Peng, J., Tang, Z., … Chan, W. K. (2016). Estimation of Hong Kong's solar energy potential using GIS and remote sensing technologies. *Renewable Energy*, *99*, 325–335.

Wu, F., Wang, X., Cai, Y., Yang, Z., & Li, C. (2012). Spatiotemporal analysis of temperature variation patterns under climate change in the upper reach of Mekong River basin. *Science of the Total Environment*, *427–428*, 208–218.

Yuan, C., & Ng, E. (2012). Building porosity for better urban ventilation in high-density cities: A computational parametric study. *Building & Environment*, *50*, 176–189.

Yuan, M., & Hornsby, K. (Eds.). (2008). *Computation and visualization for understanding dynamics in geographic domains*. Boca Raton, FL: CRC Press.

Zhu, R., Guilbert, E., & Wong, M. S. (2017). Object-oriented tracking of the dynamic behavior of urban heat islands. International *Journal of Geographical Information Science*, *31*(2), 405–424.

Zhu, R., Wong, M. S., Guilbert, E., & Chan, P. W. (2017). Understanding heat patterns produced by vehicular flows in urban areas. *Scientific Reports*, *7*, 16309.

How to cite this article: Zhu R, Guilbert É, Wong MS. Object-oriented tracking of thematic and spatial behaviors of urban heat islands. *Transactions in GIS*. 2019;00:1–19. https://doi.org/10.1111/tgis.12586